Carbon Heating Tube Rapid Heating System for Fabricating Silicon Solar Cells

Tomoyoshi Miyazaki[1,3], Go Kobayashi[2], Izumi Serizawa[2], Toshitaka Kikuchi[3], Takuma Uehara[3], Takuji Arima[3], Masahiko Hasumi[3] and Toshiyuki Sameshima[3]

[1]Techno Research., Ltd., Koganei, Tokyo, 184-0012, Japan
[2]Orc manufacturing Co., Ltd. 4896 Tamagawa, Chino, 391-0011, Japan
[3]Tokyo University of Agriculture and Technology, Graduate School of Engineering, 2-24-16, Naka-cho, Koganei, Tokyo, 184-8588, Japan
Email: tsamesim@cc.tuat.ac.jp

We report 2.45-GHz microwave heating system with a carbon heating tube (CHT) made by a 4-mm-diameter and 60-mm-long-quartz tube filled with conductive carbon particles and Ar gas at 1400 Pa set in a 300-mm-diameter-sized metal cavity. The three-dimensional finite element numerical simulation method resulted in the most effective electrical conductivity of CHT ranged from 10 to 55 S/m to absorb the microwave power. A proportional-integral-differential feedback CHT temperature control system was used to activate $1.0x10^{15}$-cm^{-2}-boron and phosphorus implanted regions in n-type crystalline silicon substrate from 1000 to 1200°C. The CHT heating at 1200°C realized decrease in the sheet resistivity to 146 Ω/sq, decrease in the density of defect states to $1.3x10^{11}$ and $9.2x10^{10}$ cm^{-2} for boron (p^+) and phosphorus (n^+) implanted surfaces, and solar cell characteristic with a conversion efficiency of 15% under illumination of air mass 1.5 at 0.1 W/cm^2.

1. Introduction

We recently proposed a new heating system with a carbon heating tube (CHT) lamp made with a quartz tube filled with carbon particles and Ar gas.[1,2] 2.45-GHz microwave at 200 W introduced into a metal cavity with the CHT was effectively absorbed by carbon in the CHT and heated it to a high temperature of 1279°C for 33 s irradiation. Moreover, we achieved the temperature control of the CHT using a proportional-integral-differential feedback (PID) circuit[3] which regulated the magnetron power source with a signal of a radiation type thermometer. Successful control of a constant temperature at 1100°C was demonstrated. We also achieved crystallization of amorphous silicon films with a high crystalline volume ratio of 0.92 and activation of boron and phosphorus atoms implanted with a dose of $1x10^{15}$ cm^{-2}. The CHT heating system would be applicable to fabrication of semiconductor devices such as thin film transistors (TFTs) and solar cells[4-7], although many heating technologies have been developed such as rapid thermal annealing, laser annealing[8,9], plasma jet annealing[10], and rapid thermal annealing.[11] It gives an advantage of no electrical wiring to the CHT lamp. It allows a simple heating system and application to heat treatment in severe environment for example high humidity atmosphere. Moreover, a capability of CHT lamp with highly thermal proof structure is realized because the junction between lamp materials and the electrode metals has always a serious problem of thermally stress-induced damage.

In this paper, we first report characterization of the electric field distribution in the cavity in the steady state during microwave irradiation analyzed by a numerical simulator constructed with the three-dimensional finite element moment method[12] to determine the effective condition of microwave absorption by the CHT. Then we demonstrate silicon solar cell fabrication using PID temperature controlled CHT heating. The effective lifetime (τ_{eff}), and solar cell characteristics are reported.

2. Experimental

2-1. CHT heating system

Figure 1 shows a schematic image of a CHT heating system. For fabricating CHTs, quartz tubes with 60-mm long and 4-mm inter diameter and 6-mm outer diameter were made. 2-μm-diameter-carbon powders with a 0.1-g weight were put in the quartz tubes, in which the packing density was controlled as 0.09 with an electrical conductivity of 55 S/m, which was determined by the previous work as the best value for heating.[13] Ar

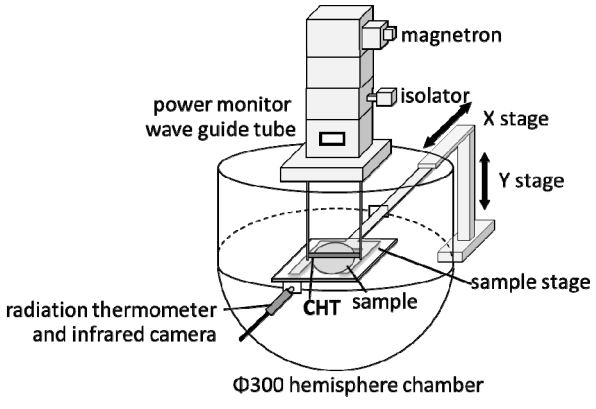

Fig. 1 Schematic image of a CHT heating system

inert gas was filled in the quartz tube at 1400 Pa. The edges of the quartz tubes were closed by thermal welding. Two quartz rods were jointed at the edges of the CHT by thermal welding to hold the CHT. A CHT was used in a heating system, which consists of a magnetron for generating 2.45-GHz microwave with an electrical power source, an isolator for blocking the reflectance of microwave backward the magnetron, a power monitor, an impedance matching box for reducing microwave reflectance, a wave-guide tube, and a cavity made by Al metals. The Microwave generated by the magnetron was introduced to the cavity by the wave guide tube via the isolator, power monitor, and impedance matching box. The cavity had a structure with a cylindrically upper part with a diameter of 300 mm and a spherically lower part to promote interferingly multiple reflection of the microwave in the cavity and to have the CHT effectively absorb the microwave. Those works resulted in a reflected power less than 4 W in the case of an input power of 500 W. In contrast, the power monitor gave the same value of the input and reflected power when the cavity had no CHT. The cavity completely reflected the microwave power. The cavity had a small window port for observing light emission from CHT heated by microwave. A thermometer detecting 900-nm wavelength radiation light CHINO IR-FAS was used to monitor the temperature of the CHT in real time. The detection lower limit of the thermometer was about 550ºC. The analog voltage signal of the thermometer is monitored in real time by a PID circuit controller which was installed with a plan of temperature increasing and decreasing ratios, a target temperature and its duration in its memory in advance. The controller sent a signal to the power source of the magnetron to increase or decrease the microwave power for coinciding the CHT temperature with the initial temperature plan. A mechanically moving stage formed by quartz pipes was also installed in the cavity to move a sample just below the CHT.

2-2. Numerical calculation

The electric field distribution in the cavity in the steady state during microwave irradiation was numerically analyzed by a simulator constructed with the three-dimensional finite element moment method combined with the Cholesky decomposition. The grid system of the cavity and waveguide was formed with the equilateral-triangle elements with the sides ranging from 1 to 4 mm for the numerical calculation. They were assumed as perfect electric conductor which reflects completely the microwave. The CHT grid was formed with 1-mm-side-equilateral-triangle elements. The electrical conductivity of carbon was widely changed from 0.1 to 10000 S/m to find an effective condition of microwave absorption by the CHT. The calculation of electric field distribution in the cavity was also conducted in the case of no CHT.

2-3. Solar cell fabrication

4-inch-diameter 500-μm-thick 17-Ωcm n-type silicon substrates coated with 100-nm-thick thermally grown SiO_2 layers were prepared. The ion implantation of boron atoms was conducted with a dose of $2x10^{15}$ cm^{-2} at 25 keV to the top silicon surface of the substrates. Phosphorus atoms with $2x10^{15}$ cm^{-2} at 75 keV was also implanted to the rear surface. The boron and phosphorus atoms with a dose of $1.0x10^{15}$ cm^{-2} were effectively incorporated in the top and rear silicon surface regions. The samples were cut to 4 sectored pieces. They were placed in the heating system just below the CHT and moved at 0.12 mm/s. The CHT temperature was controlled by PID feedback method at 1000, 1100, and 1200ºC. After heating, the thermally grown SiO_2 layer was removed using hydro-fluoric acid. To estimate the sheet resistivity and effective minority carrier lifetime τ_{eff}, we measured the 9.35 GHz microwave transmittance of the samples in dark field and 635-nm-light illumination.[14] Comb-type Al electrodes were formed on the top surface and the rear sur-face was entirely coated with Al electrodes by vacuum evaporation. 100-nm-thick AlO_x layers was subsequently deposited on the top surfaces as anti-reflection layer. The samples were heated in H_2O vaper at 0.8 MPa at 230ºC for 3 h to decrease defect states in the doped regions.[15] The electrical current density as a function of applied voltage (J–V) was measured under illumination of air mass (AM) 1.5 light at 0.1 W/cm^2.

3. Results and discussion

Figure 2 shows calculated cross-sectional electric field distributions in the cavity (a) with no CHT, (b) with 55-S/cm-CHT placed at the central region of the cavity, and (c) with the 10000-S/cm-CHT placed at the same position as (b) when the 200 W microwave was continuously introduced in the cavity. The cavity and CHT surface outlines were traced by sold black curves. The calculation resulted in the standing wave of the electric field in every case because of the three-dimensional Fresnel interference effect observed in the cavity. The numerical calculation resulted in existence of a high electric field intensity ranging from 1000 to 6000 kV/m in the case of no CHT, as shown in Fig. 2(a). In contrast, the electric field intensity was very low in the case of the cavity with the CHT. The most of region of the cavity had the electric field ranged from 1 to 6 kV/m, as shown in Fig. 2(b). It was reduced to at least 0.1% of the initial intensity of the cavity

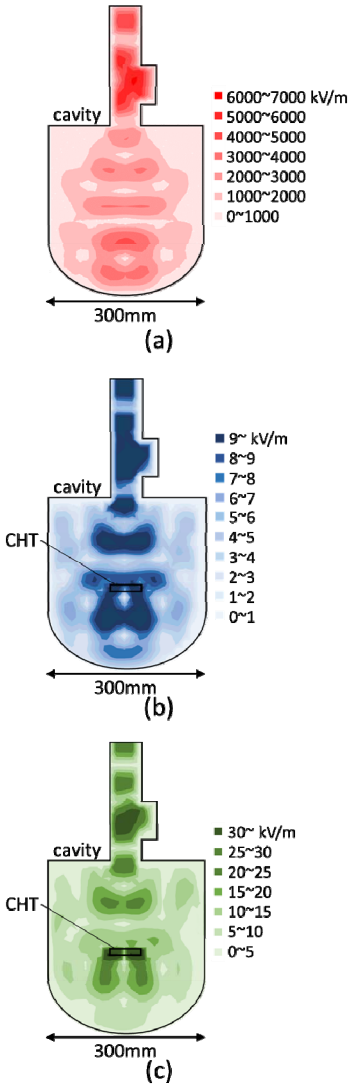

Fig. 2 Calculated cross-sectional electric field distributions in the cavity (a) with no CHT, (b) with 55-S/m-CHT placed at the central region of the cavity, and (c) with the 10000-S/m-CHT when the 200 W microwave was continuously introduced in the cavity.

space without CHT. On the other hand, the electric field intensity distributed from 10 to 60 kV/m in the case of 10000-S/m-CHT, as shown in Fig. 2(c). These calculated results indicate that the cavity effectively accumulated the microwave power, and that the microwave power in the cavity was almost completely absorbed by the 55-S/m-CHT. Absorption of microwave power depends on the electrical conductivity. A CHT with a very high electrical conductivity (a high packing density of carbon particles) is not suitable because of high reflectivity caused by a high extinction coefficient. Figure 3 shows the average electric field intensity in the cavity space as a function of the electrical conductivity of the CHT. Although the average electric field intensity was very high of 1173 KV/m in the case of no CHT, it was decreased by installing CHTs, as shown in Fig. 3. The minimum average electric field intensity was 5 kV/m when the electrical conductivity ranged between 10 and 55 S/m. This means that the effective absorption of the microwave power by CHT reduced the electric field intensity in the cavity. The average electric field intensity gradually increased as the electrical conductivity further increased. The calculation supports experimental results of low microwave refection from the cavity and effective heating of the CHT.[1,2)]

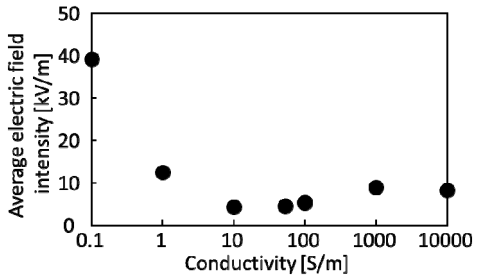

Fig. 3 Average electric field intensity in the cavity space as a function of the electrical conductivity of the CHT

Figure 4 shows (a) the sheet resistivity of the samples and (b) τ_{eff} in the case of 635 light illumination to the boron (solid circles) and phosphorus (open circles) implanted surfaces as functions of CHT heating temperature. Although, the sheet resistivity of as-implanted sample was high of 626 Ω/sq caused by 9.35-GHz-microwave absorption by the low concentration of the electron carriers in the silicon bulk, it decreased from 215 to 146 Ω/sq as the CHT heating temperature increased from 1000 to 1200°C. This experimental result shows that the activation in implanted region and carrier generation were successfully achieved by CHT heating. τ_{eff} was also increased by CHT heating, although it was low of 1.1×10^{-5} and 8.1×10^{-6} s in the cases of light illumination to the as-boron and as-phosphorus implanted surfaces. The 1200°C-CHT-heating achieved 2.0×10^{-4} and 2.2×10^{-4} s in the cases of 635-nm-light

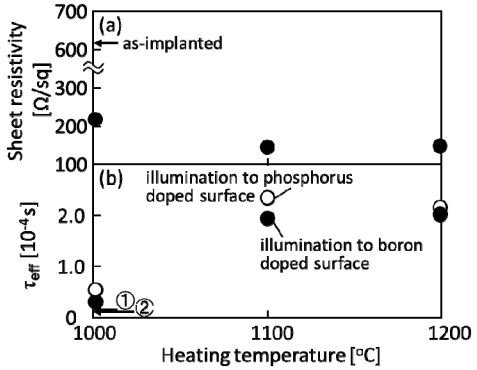

Fig. 4 (a) Sheet resistivity of the samples and (b) τ_{eff} in the case of 635 light illumination to the boron (solid circles) and phosphorus (open circles) implanted surfaces as functions of CHT heating temperature. Arrows ① and ② represent τ_{eff} in the cased of light illumination to the boron and phosphorus implanted surfaces.

illumination to the boron and phosphorus implanted surfaces. This means that defect states caused by ion implantation were effectively reduced. Our numerical analysis resulted in that the recombination defect densities were $1.3x10^{11}$ and $9.2x10^{10}$ cm^{-2} for boron (p^+) and phosphorus (n^+) implanted surfaces.[16)]

Figure 5 shows characteristics of solar cells fabricated with CHT heating at temperatures of 1000, 1100, and 1200°C. The AM 1.5 light illumination realized typical photovoltaic characteristics for every solar cell sample. The short circuit current density and open circuit voltage increased as the CHT heating temperature increased. The 1200°C heating realized the best performance with the short circuit current density, open circuit voltage, fill factor, and conversion efficiency of 39 mA/cm^2, 0.55 V, 0.69, and 15%, respectively. These results indicate that the temperature-controlled CHT heating has a capability of activating dopant-implanted regions, reducing the defect states, realizing high performance silicon solar cells.

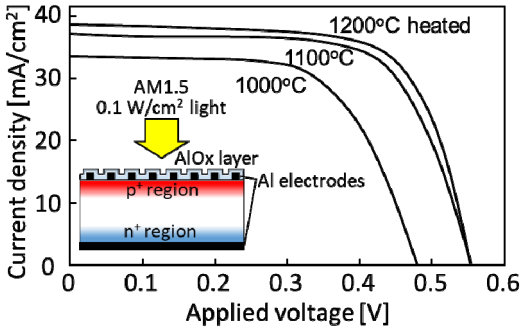

Fig. 5 Characteristics of solar cells fabricated with CHT heating temperatures of 1000, 1100, and 1200°C.

4. Conclusions

Silicon solar cells were fabricated by the CHT heating to form the pn junction in 500-μm-thick single crystalline n-type silicon substrates. $1.0x10^{15}$ cm^{-2} boron and phosphorus ion implanted regions were heated from 1000 to 1200°C by the PID feedback CHT heating equipment which consisted of 2.45-GHz microwave irradiation into 300-mm-diametered semispherical metal cavity to accumulate the microwave which was effectively absorbed by CHT made by a 4-mm-diameter and 60-mm-long quartz tube filled with conductive carbon particles at an average electrical conductivity of 55 S/m in Ar gas at 1400 Pa. The three-dimensional finite element numerical simulation method resulted in the most effective electrical conductivity of CHT range from 10 to 55 S/m to absorb the microwave power. The sheet resistivity decreased to 146 Ω/sq by 1200°C heating and the density of defect states also decreased to $1.3x10^{11}$ and $9.2x10^{10}$ cm^{-2} for boron (p^+) and phosphorus (n^+) implanted surfaces. Via formation of Al metal electrodes and AlO_x-antireflection layer resulted in solar cell characteristics with the short circuit current density, open circuit voltage, fill factor, and conversion efficiency of 39 mA/cm^2, 0.55 V, 0.69, and 15%, respectively, under illumination of air mass 1.5 at 0.1 W/cm^2.

Acknowledgments

This work was partially supported by Japan Science and Technology Agency ASTEP (No. AS3015022S).

References

1) T. Miyazaki, G. Kobayashi, T. Sugawara, T. Kikuchi, M. Hasumi and T. Sameshima: AMFPD, 2018, 1-4.

2) T. Sameshima, T. Miyazaki, G. Kobayashi, T. Arima, T. Kikuchi, T. Uehara, T. Sugawara, M. Hasumi and I. Serizawa: IEEE Access, 7 (2019) 23798-23805.

3) Aidan O'Dwyer: Handbook of PI and PID Controller Tuning Rules, 3rd ed., London, Imperial College Press, 2009, 4-17.

4) S. Uchikoga and N. Ibaraki: Thin Solid Films, 383 (2001) 19.

5) S. Inoue, K. Sadao, T. Ozawa, Y. Kobashi, H. Kwai, T. Kitagawa and T. Shimoda: Tech. Dig. IEDM, 2000, p. 197.

6) K.Shibata and H. Takahashi: AMFPD, 2001, p. 219.

7) S. M. Sze: Semiconductor Devices, Wiley, New York, 1985.

8) R. F. Wood and C. E. Giles: Rhys. Rev. B23 (1981) 2923.

9) T. Sameshima, S. Usui and M .Sekiya: IEEE Electron Device Lett. 7 (1986) 276.

10) S. Higashi, H. Kaku, H. Murakami, S. Miyaszaki, H. Watakabe, N. Ando and T. Sameshima: Jpn. J. Appl. Phys. 44 (1989) 108.

11) G. Mannino: Appl. Phys. Lett. 78 (2001) 889.

12) J. H. Richmond: IEEE Trans. Antennas & Propagation, Vol. AP-14, No.6, (1966) pp.782-786.

13) S. Kimura, K. Ota, M. Hasumi, A. Suzuki, M. Ushijima and T. Sameshima: Appl. Phys. A. Vol. 122 (2016) 695-1-9.

14) T. Sameshima, T. Motoki, K. Yasuda, T. Nakamura, M. Hasumi and T. Mizuno: Jpn. J. Appl. Phys. 54 (2015) 081302-1-6.

15) K. Sakamoto and T. Sameshima: Jpn. J. Appl. Phys. 39 (2000) 2492-2496.

16) T. Sameshima, J. Furukawa, T. Nakamura, S. Shigeno, T. Node, S. Yoshidomi and M. Hasumi: Jpn. J. Appl. Phys. 53 (2014) 031301-1-6.